Advanced Ultrasound Techniques for Pediatric Imaging

Misun Hwang, MD,[a] Maciej Piskunowicz, MD, PhD,[a,b] Kassa Darge, MD, PhD[a]

Ultrasound has become a useful tool in the workup of pediatric patients because of the highly convenient, cost-effective, and safe nature of the examination. With rapid advancements in anatomic and functional ultrasound techniques over the recent years, the diagnostic and interventional utility of ultrasound has risen tremendously. Advanced ultrasound techniques constitute a suite of new technologies that employ microbubbles to provide contrast and enhance flow visualization, elastography to measure tissue stiffness, ultrafast Doppler to deliver high spatiotemporal resolution of flow, three- and four-dimensional technique to generate accurate spatiotemporal representation of anatomy, and high-frequency imaging to delineate anatomic structures at a resolution down to 30 μm. Application of these techniques can enhance the diagnosis of organ injury, viable tumor, and vascular pathologies at bedside. This has significant clinical implications in pediatric patients who are not easy candidates for lengthy MRI or radiation-requiring examination, and are also in need of a highly sensitive bedside technique for therapeutic guidance. To best use the currently available, advanced ultrasound techniques for pediatric patients, it is necessary to understand the diagnostic utility of each technique. In this review, we will educate the readers of emerging ultrasound techniques and their respective clinical applications.

Ultrasound in which advanced techniques are used can enhance the diagnostic sensitivity of conventional grayscale and color Doppler ultrasound while offering additional functional information. In contrast-enhanced ultrasound (CEUS), intravascular microbubble agents are used to highlight perfusion abnormalities associated with various pathologies, including organ injury and residual tumors, which would otherwise be challenging to identify with conventional ultrasound.[1–3] The enhanced diagnostic sensitivity of CEUS can negate the need for further high-cost, cross-sectional imaging requiring sedation.

Elastography is another functional ultrasound technique that allows for the quantification of tissue stiffness, which reflects tissue composition and/or architecture, edema, injury, and perfusion. The technique provides a quantitative or semiquantitative measure of the tissue evaluated. Two main types of elastography include strain and shear elastography. Strain elastography can produce a semiquantitative measure of tissue stiffness by detecting axial displacements arising from either manual compression or internal physiologic motion (eg, respiration and heartbeat). Shear-wave elastography applies high-intensity pulses to deform the tissue and produce laterally propagating shear waves that can be used to quantify stiffness. Elastography is approved by the Food and Drug Administration (FDA) for the evaluation of all

abstract

[a]*Department of Radiology, Children's Hospital of Philadelphia and Perelman School of Medicine, University of Pennsylvania, Philadelphia, Pennsylvania; and* [b]*Department of Radiology, Medical University of Gdansk, Gdańsk, Poland*

Dr Hwang conceptualized and wrote the manuscript; Drs Piskunowicz and Darge contributed to the writing and image acquisition; and all authors approved the final manuscript as submitted and agree to be accountable for all aspects of the work.

This trial has been registered at www.clinicaltrials.gov (identifiers NCT03549507 and NCT03549520).

DOI: https://doi.org/10.1542/peds.2018-2609

Accepted for publication Nov 19, 2018

Address correspondence to Misun Hwang, MD, Section of Neonatal Imaging, Division of Body Imaging, Department of Radiology, Children's Hospital of Philadelphia, Perelman School of Medicine, University of Pennsylvania, 3401 Civic Center Blvd, Philadelphia, PA 19104. E-mail: hwangm@email.chop.edu

PEDIATRICS (ISSN Numbers: Print, 0031-4005; Online, 1098-4275).

FINANCIAL DISCLOSURE: Dr Hwang has received funding from the National Institutes of Health KL2 award. Dr Piskunowicz has received funding from National Science Center grant DEC-2012/05/B/NZ5/01554. Dr Darge has financial relationships with Bracco Diagnostics Inc, Lantheus Medical Imaging, Philips Healthcare, and Siemens Healthineers.

FUNDING: Funded by the National Institutes of Health KL2 award and Radiological Society of North America Research Scholar Grant (Dr Hwang) and National Science Center grant DEC-2012/05/B/NZ5/01554 (Dr Piskunowicz). Funded by the National Institutes of Health (NIH).

POTENTIAL CONFLICT OF INTEREST: The authors have indicated they have no potential conflicts of interest to disclose.

To cite: Hwang M, Piskunowicz M, Darge K. Advanced Ultrasound Techniques for Pediatric Imaging. *Pediatrics*. 2019;143(3):e20182609

STATE-OF-THE-ART REVIEW ARTICLE

abdominal organs in pediatric patients.

Furthermore, improvements in three-dimensional (3D) ultrasound techniques enable accurate quantification and delineation of anatomic structures for improved diagnosis and surgical guidance. The integration of four-dimensional (4D) ultrasound, with the fourth dimension representing time, allows for 3D depiction of moving objects, such as the heart valves in echocardiography. There is ongoing research to simultaneously scan the whole-organ volume without reconstructive postprocessing, which, if successful, will significantly advance the clinical potential of 3D ultrasound.[4]

Ultrafast Doppler (UfD) is an advanced Doppler technique with significantly higher temporal resolution than conventional Doppler (up to 100 000 frames per second as opposed to 50 frames per second), offering real-time blood volume changes shown to correlate with neuronal activation.[5] Moreover, high-resolution imaging in which a frequency of up to 70 MHz (compared with conventional imaging with a frequency of up to 15 MHz) is used can enhance the diagnostic sensitivity of various dermatologic, neuromuscular, vascular, and other superficial pathologies because of the improved resolution in the region close to the transducer.

In this review, we will highlight recent advancements in anatomic and functional ultrasound techniques that have the potential to significantly improve the diagnostic and therapeutic potential of ultrasound. Our goal for the review is to educate the readers of the availability of these emerging ultrasound techniques and their potential clinical applications.

CEUS

The ultrasound contrast agents are gas-containing, phospholipid-encapsulated microbubbles of 2 to 3 μm in size (compared with 7–8 μm of red blood cells) that generate an increased ultrasound signal because of a high acoustic impedance mismatch. Lumason (Bracco Diagnostics Inc, Monroe, NJ), sulfur hexafluoride gas-filled microbubbles encapsulated by phospholipids, was approved for characterization of focal liver lesions and evaluation of vesicoureteral reflux by the FDA in 2016.[6] The technique requires injection of the manually reconstituted contrast agent into a peripheral vein and detecting the signal reflected from the microbubbles flowing in the vessels. Its safety profile is much superior to computed tomography (CT) and MRI contrast agents.[7,8] The contrast agent is primarily exhaled and not renally cleared. Because of the excretion through the lungs, the contrast agent can be safely given to patients with renal insufficiency. In addition, it allows for an ultrasound study with contrast, avoiding the radiation of CT and the sedation needed for MRI. These serve as major advantages in pediatric imaging. CEUS is also lower in cost compared with CT or MRI.

Benign Focal Parenchymal Lesions

The main benefit of CEUS in small children is the ability to diagnose certain benign focal lesions, such as hemangioma, focal nodular hyperplasia, or fatty infiltration, obviating the need for expensive radiation or sedation requiring, at times, lengthy cross-sectional imaging. Hemangiomas have a characteristic centripetal pattern of enhancement, with avid peripheral enhancement and progressive mild central enhancement, which can be diagnosed with CEUS alone.[9] Grayscale ultrasound and color Doppler findings of these benign focal lesions can be puzzling because the dynamic wash-in and wash-out pattern seen with CEUS cannot be obtained.

We present a challenging case of a large congenital hepatic hemangioma diagnosed with CEUS on initial scanning that would have otherwise been a diagnostic challenge with conventional ultrasound alone (Fig 1). The lesion demonstrated heterogeneous echotexture and an indeterminate color Doppler signal. With a CEUS scan, however, the lesion proved to have avid enhancement in the periphery, to the same degree as the aorta, and partial centripetal filling on day 2 of life (Supplemental Video 1). The diagnosis of hemangioma was made at the time. Subsequent scans obtained monthly until 8 months revealed progressive irregular enhancement of the periphery of the lesion, still enhancing avidly as the aorta, with an increase in the size of the lesion. MRI obtained at 8 months of life revealed the same peripherally avid enhancement pattern seen on CEUS acquired the same month. A biopsy was performed because of the increasing size of the lesion, and the diagnosis of congenital hemangioma was made. Subsequent CEUS of the lesion performed 2 months after the MRI revealed a slight decrease in the size of the lesion and a smoother echotexture and enhancement pattern, most compatible with rapidly involuting congenital hemangioma.

The above case represents an example in which increased CEUS experience and familiarity within the medical community would have prevented a biopsy, which is not without risks, especially because the lesion was seen to regress in size at 10 months of life. Noninvasive monitoring of the lesion with CEUS would have been sufficient. It also highlights the value of CEUS in reducing the number of MRI scans and associated sedation, which has been associated with neurotoxic effects in the developing brain.[10,11] Additionally, magnetic resonance contrast administration is posing a challenge because of the gadolinium

accumulation in the body. Further benign CEUS enhancement characteristics include well-defined peripheral and/or central vascular pattern (ie, benign lymph nodes, hyperplastic thyroid nodules, focal nodular hyperplasia, and splenic hamartoma), delayed wash out (ie, liver regenerative nodules), and lack of enhancement (ie, hemorrhage, cyst, column of Bertin, and calyceal diverticulum). In summary, CEUS can serve as a diagnostic and/or monitoring tool for many benign lesions without the need for additional imaging and the possibility of a bedside examination.

Malignant Focal Lesions

CEUS permits real-time imaging of dynamic perfusion with high temporal resolution and quantitative analysis of in flow and out flow of the microbubbles through the vessels and within the lesion. Because the vascularization pattern of benign and malignant lesions is different, CEUS can be a useful tool in distinguishing the 2.[12] On CEUS, most malignant lesions reveal fast arrival of the contrast agent (wash in) during the arterial phase followed by rapid wash out. The quick wash-out phenomenon is one of the most characteristic features of a malignant lesion because of a nearly complete arterial blood supply and abnormal arterio-venous shunts. Accurate assessment of tumor vascularity is possible because of

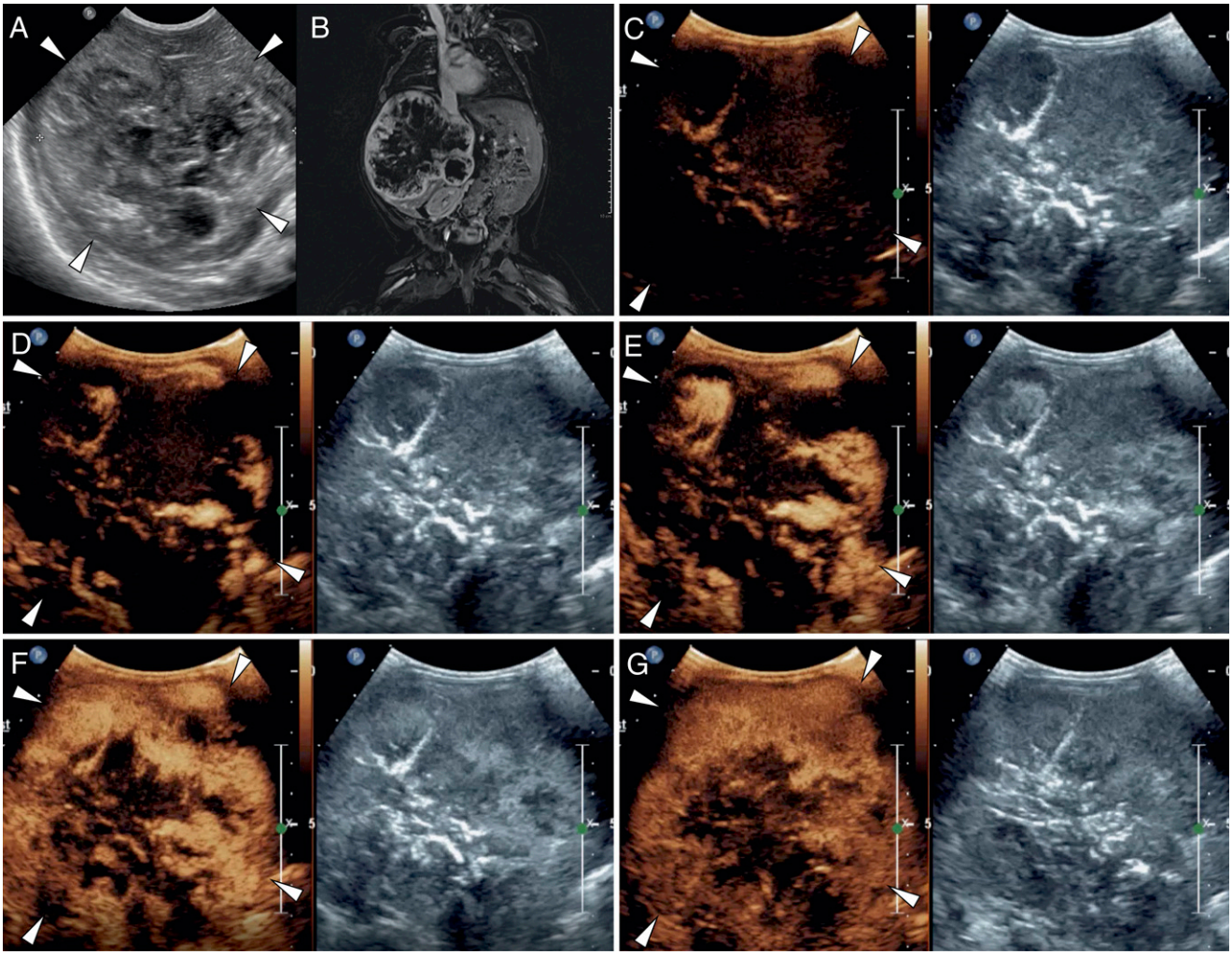

FIGURE 1

A large liver hemangioma shown with grayscale ultrasound, CEUS, and MRI, and CEUS images demonstrating centripetal enhancement over time. A, Grayscale ultrasound image of a hemangioma on the initial scan 8 months before the CEUS (C–G) and MRI (B) acquisition. B, Coronal, fat-saturated contrast-enhanced MRI image obtained a few days after the CEUS scan showing a large liver hemangioma with irregular peripheral rim enhancement. C, CEUS image of the lesion (white arrowheads) shown in contrast mode (left) and grayscale mode (right) before microbubble administration. The image is dark, as expected, before microbubble administration on contrast mode. Note the irregular streaks of bright signals within the lesion in the absence of microbubbles, likely due to internal calcifications. D, CEUS image of the lesion is shown at 10 seconds after intravenous microbubble administration. E, CEUS image of the lesion is shown at 12 seconds after administration. F, CEUS image of the lesion is shown at 15 seconds after administration. G, CEUS image of the lesion is shown at 95 seconds after administration.

retention of microbubbles within the intravascular space in contrary to increased permeability of iodinated and gadolinium-based contrast agents.[13–15]

The potential spectrum of the clinical application of CEUS in pediatric oncology is broad. Immediate exclusion of malignancy without the need to wait for further imaging studies substantially reduces the stress for parents and their child. In terms of biopsy guidance, CEUS could identify areas of a necrotic versus viable tumor so as not to result in false-negative results (Fig 2). With the technique, serial quantitative estimation of tumor vasculature is feasible for assessment of response to anticancer treatment (Fig 3). Lastly, CEUS could reduce a number of oncologic follow-up examinations with the use of ionizing radiation and/or general anesthesia. In a study in which the authors evaluated the utility of CEUS in children, it was shown that CEUS substantially decreased the need for further evaluation with MRI or CT.[16]

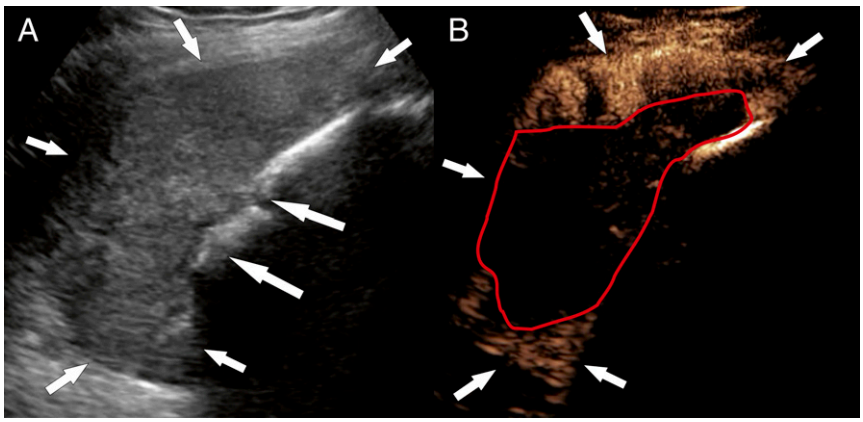

FIGURE 2
CEUS of pelvic osteosarcoma in a 13-year-old boy was obtained for biopsy guidance. A, Grayscale ultrasound of pelvic osteosarcoma (short white arrows) of heterogeneous echogenicity reveals bone destruction, (long white arrows) as evidenced by a disruption of the echogenic line representing the cortex of the adjacent ilium. B, CEUS of pelvic osteosarcoma (short white arrows) at 14 seconds after contrast administration with a visible large region of necrosis (red circumscribed area) and enhancing tumor tissue on the periphery.

Organ Perfusion

The degree of microbubble enhancement is reflective of organ perfusion and viability, and CEUS may be used for diagnosis of organ ischemia, injury, or death. CEUS can depict varying degrees of brain injury, as can be seen with postinjury hyperperfusion, and the evolution of reperfusion response has important prognostic implications (Fig 4, Supplemental Video 2). For infants who are critically ill with significant brain injury, timely performance of either 4-vessel cerebral angiography or radionuclide cerebral blood flow studies for diagnosis of brain death is not easy. If further validated against the gold standard examinations, CEUS has the potential to serve as an alternate tool for diagnosis of brain death.[17] Moreover, the bedside use of CEUS for diagnosis of trauma has shown much potential because of the portability and repeatability of the examination combined with superior diagnostic sensitivity compared with conventional ultrasound.[18,19] In the case of necrotizing enterocolitis, CEUS can serve as a complementary tool for

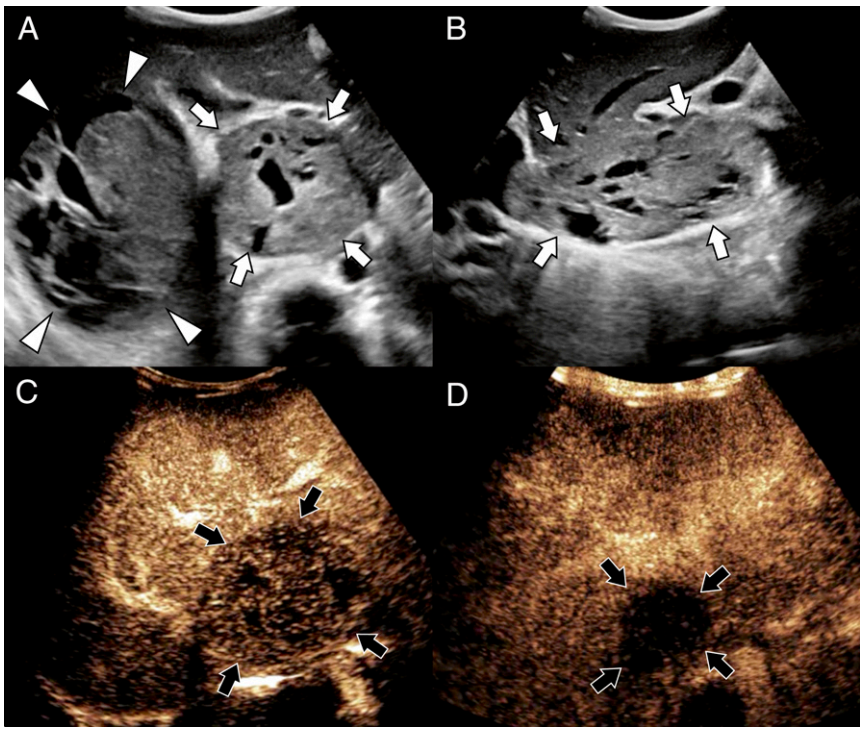

FIGURE 3
CEUS of the nephroblastoma in a 3-year-old boy extending into the right atrium and inferior vena cava was obtained before and after therapy to assess for treatment response. A, Transverse grayscale ultrasound of the nephroblastoma in the right atrium revealing solid cystic echotexture (arrowheads) and extending into the inferior vena cava (white arrows). B, Sagittal grayscale ultrasound revealing extension of the tumor thrombus from the inferior vena cava into the right atrium (white arrows). C, CEUS of the vascularized tumor thrombus in the inferior vena cava (black arrows) before treatment is shown. D, CEUS of the tumor thrombus in the inferior vena cava after 2 cycles of chemotherapy revealing marked decreased vascularization and diameter (black arrows).

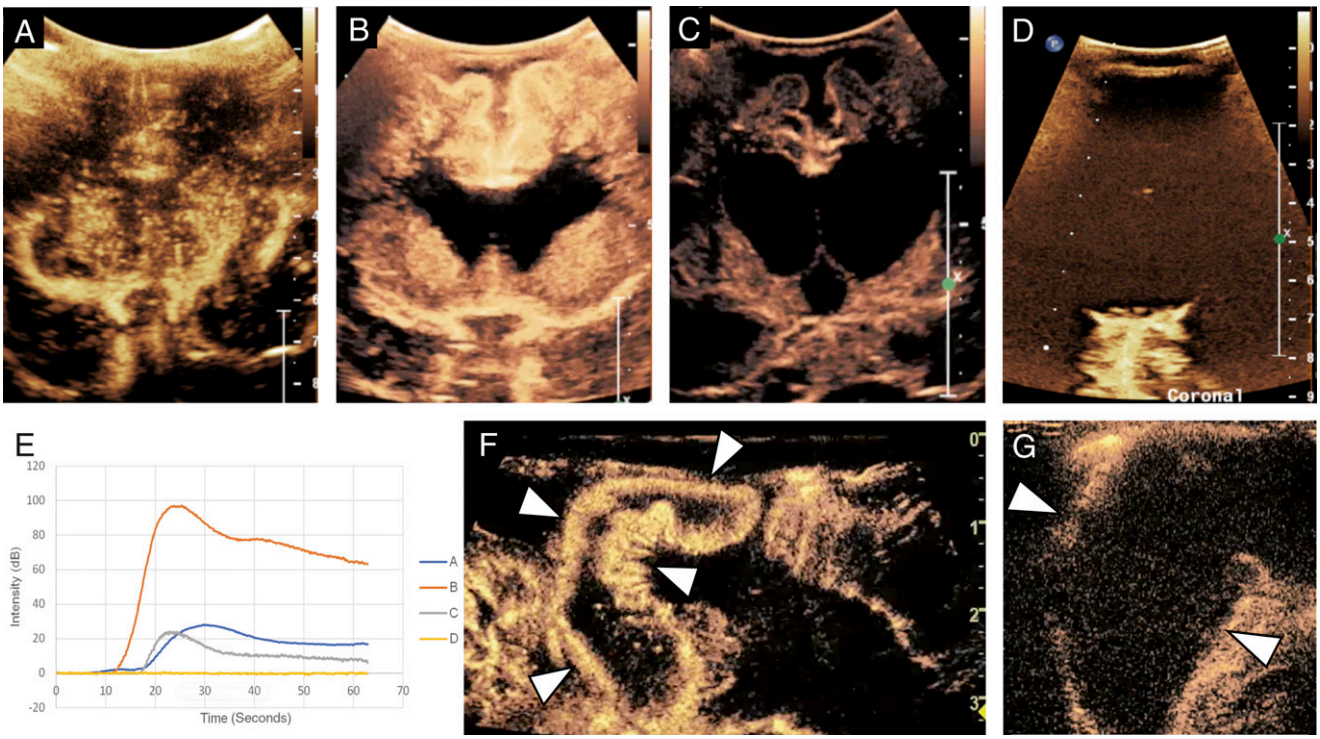

FIGURE 4

CEUS images of brain and bowel perfusion are shown. A, Midcoronal brain CEUS image of a normal 1-month-old boy obtained at 15 seconds after microbubble administration revealing relative hyperperfusion to the central gray nuclei compared with the remainder of the brain, which is expected for that age. Normal-sized ventricles and brain volume for age are seen. B, A midcoronal brain CEUS image of a 10-month-old girl after cardiac arrest status post extracorpreal membrane oxygenation. Midcoronal brain CEUS obtained15 seconds after microbubble administration reveals marked increased perfusion to the cortical and subcortical gray and white matter, which is not typically seen in normal neonates and infants. Note also the hyperperfusion to the central gray nuclei, which is slightly higher than expected for that age. C, A midcoronal brain CEUS image of the same 10-month-old girl obtained 1 week after the examination obtained in (B), with the image acquired at 15 seconds after microbubble administration. Compared with the previous brain CEUS examination (B), significant overall decreased perfusion to the brain is noted, likely due to evolving injury, compared with the normal brain CEUS (A). Less avid perfusion to the central gray nuclei and cortex is demonstrated, as evidenced on the time intensity curve analysis (E). D, Midcoronal brain CEUS image of a 6-month-old boy 3 hours after cardiac arrest of unknown etiology reveals a near absent brain perfusion and to-and-fro flow in the avidly enhancing extracranial vessels. Note that the images (A, B, and D) were obtained with an EPIQ scanner (Philips Healthcare, Bothell, WA) and C5-1 transducer with settings of 12 Hz and a mechanical index of 0.06. Image (C) was obtained with Aplio i800 (Toshiba Medical Systems Corp, Tokyo, Japan) and an i8-C1 transducer with settings of 9 Hz and a mechanical index of 0.06. E, Normalized time intensity curve graph of the wash in of microbubbles into the brain in patients (A–D), with y-axes representing changes in signal intensity (decibels) and x-axes representing time in seconds. Note the marked hyperperfusion in the patient (B) and absent perfusion in near brain death (D). F, Bowel CEUS of a 39-day-old, formerly premature girl with necrotizing enterocolitis reveals a hyperemic bowel segment (white arrowheads). G, A bowel CEUS of a 1-day-old, formerly premature girl found to have complete bowel ischemia with no enhancement of the bowel and surrounding mesentery (white arrowheads), likely due to prenatal insult.

assessing bowel perfusion and identifying bowel ischemia, the diagnosis of which would otherwise be delayed because of the presence of an oscillator causing a false color Doppler signal or the absence of flow in the bowel wall misconstrued as technical limitations of color Doppler (Fig 4, Supplemental Video 3).

In addition, CEUS can be used to assess the degree of inflammation or fibrosis and/or scarring. In Crohn disease, the discernment of fibrotic versus inflammatory bowel strictures has important clinical implications. Inflammatory bowel strictures respond better to anti-inflammatory medications, whereas fibrotic strictures may benefit from surgical resection. Although MRI should be the gold standard for the diagnosis of Crohn disease, its use for routine monitoring of the diseased bowel segment is limited in children because of high cost and sedation needs. In this setting, CEUS may be used for serial monitoring of therapeutic response and evolution of the disease during clinic visits and potentially serve as a comparable tool to MRI by providing a quantifiable dynamic perfusion pattern of the diseased bowel segment. If combined with elastography, an advanced ultrasound technique that can assess tissue stiffness, CEUS may improve our understanding and management of diseased bowel segments with varying degrees of fibrosis and inflammation.[20,21]

Vesicoureteral Reflux

In the 1990s, contrast-enhanced voiding urosonography (ceVUS) was

introduced as a safe, radiation-free alternative to voiding cystourethrography (VCUG) in children. The technique consists of administration of microbubbles through a urinary catheter and evaluation for vesicoureteral reflux with ultrasound (Fig 5). Since then, thousands of children have been evaluated with ceVUS for vesicoureteral reflux, with a favorable safety profile. In a study of 1010 children ages 15 days to 17.6 years evaluated with ceVUS, no serious adverse event occurred, and only a few minor events occurred, likely because of catheterization.[22] More recent prospective clinical trials in which the authors compared the diagnostic sensitivity of VCUG and ceVUS revealed comparable[23] or superior[24] diagnostic sensitivity of ceVUS in comparison with the conventional VCUG. The higher sensitivity of ceVUS in the detection of vesicoureteral reflux and the ability to conduct a detailed evaluation of the urethra have enabled ceVUS to replace VCUG.

ELASTOGRAPHY

Ultrasound elastography is a functional imaging technique in which tissue stiffness can be inferred and quantified by studying the alterations in speed of traveling ultrasound waves. The stiffer the tissue, the faster a wave travels. Ultrasound elastography was initially developed by the food industry to evaluate the stiffness, or maturity, of cheeses.[25] Since its introduction in 2002 for assessment of liver fibrosis,[26] rapid improvements in the technique has resulted in the ability to accurately identify different stages of liver fibrosis for application in a variety of disorders, including nonalcoholic fatty liver disease and metabolic, autoimmune, and veno-occlusive diseases.[27–36]

In brief, there are 2 main types of ultrasound elastographies: shear-wave and strain elastography (Fig 6). The former is used to quantify absolute tissue stiffness by applying high-intensity pulses and detecting laterally propagating waves as a result of tissue deformation. The latter is a semiquantitative technique in which manual compression or internal physiologic motion, such as the heartbeat, results in axial displacements reflective of tissue stiffness. The strain elastography is semiquantitative because the exact force used to generate tissue displacement is unknown, but relative tissue stiffness (ie, stiffness of a lesion compared with the surrounding area) can be obtained in the interrogated region of interest.

One of the major benefits of elastography is the reduced need for an invasive liver biopsy, which oftentimes requires moderate sedation to general anesthesia in small children and is associated with a 6% complication risk (up to 0.1% life-threatening).[37] Although a biopsy is accepted as the gold standard, it has its own limitations, including sampling error and substantial variability in the staging of histopathologic fibrosis of up to 33% in previous literature.[38] There is also no validated histologic scoring system of liver fibrosis for the pediatric population.

Although further research is needed, elastography may be used to diagnosis other pathologies, including severe brain injury,[39] fibrotic bowel segment,[21,40] and renal fibrosis.[41] Noninvasive inference of the severity of brain injury is of clinical importance because invasive intracranial pressure measurements are not without risks. Severe anoxic brain injury can be quantitatively detected by elastography as an increase in stiffness due to brain edema, although the exact biochemical and physiologic basis of such elasticity change in the affected tissue warrants further research.[39] Close monitoring of brain injury also permits timely institution of neuroprotective and/or adjunct therapies for improved outcome. In the setting of Crohn disease, in which distinction between fibrosis and inflammation is critical to

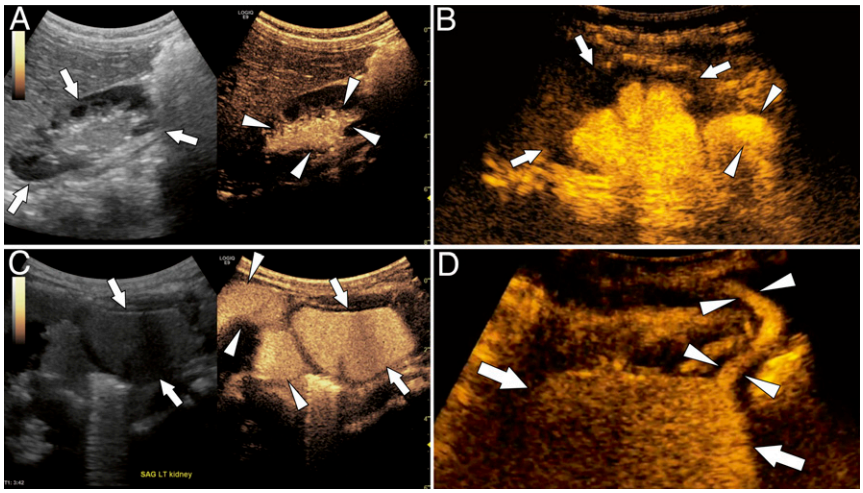

FIGURE 5

ceVUS images are shown. A, Side by side sagittal grayscale and corresponding ceVUS image of the right kidney (white arrows) of a 19-month-old boy revealing grade 2 reflux into the renal pelvis (white arrowheads). B, Sagittal ceVUS image of the right kidney (white arrows) with grade 4 reflux into the dilated renal pelvis and calyces (white arrowheads) in a 16-month-old boy. C, Microbubble-filled tortuous megaureter (arrowheads) and bladder (white arrows) in a 3-week-old boy. D, Sagittal ceVUS image of the microbubble-filled urinary bladder (white arrows) and urethra (white arrowheads) in an 8-month-old boy during the voiding phase.

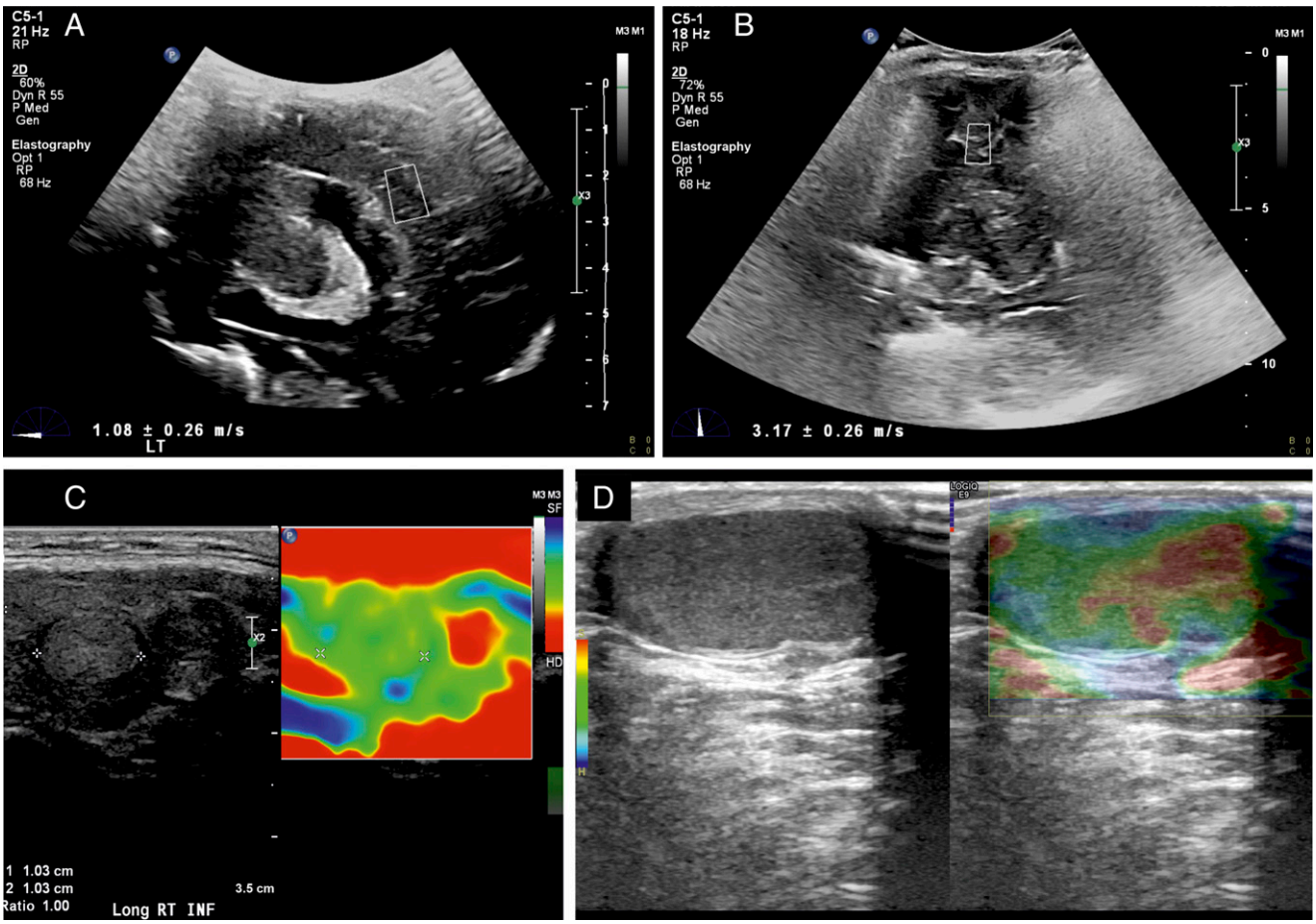

FIGURE 6

Shear-wave and strain elastography images are shown. A, A rectangular cursor is placed in the cortex of the brain of a normal neonate on a sagittal plane for shear-wave elastography measurement, here shown as 1.08 ± 0.26 m/s. B, Similar shear-wave elastography measurement of the periventricular gray-white matter in an infant after anoxic brain injury reveals a markedly elevated elastography measurement of 3.17 ± 0.26 m/s. C, A solid, isoechoic thyroid nodule depicted on grayscale ultrasound (left) and strain elastography (right), with the strain elastography revealing mild increased stiffness as noted by the green color (blue noting soft and red noting hard). D, A normal testis shown in grayscale ultrasound (left) and strain elastography mode (right) reveals slightly stiffer tissue (this time denoted by blue/green) close to the echogenic band of connective tissue across the testis, so-called mediastinum testis, compared with the adjacent softer tissue (red). Note that depending on the system settings, color representation of tissue stiffness may differ.

determining a surgical versus anti-inflammatory medical approach, elastography may be of importance in the diagnosis of inflammatory and/or fibrotic bowel strictures. In patients with chronic kidney disease, elastography may be of prognostic value in identifying those at risk for renal function deterioration.[41]

UFD

UfD is an advanced Doppler technique with a high temporal resolution of >100 000 frames per second compared with the typical 50 frames per second used in conventional color Doppler imaging (Fig 7).[42] The technique sends out a plane wave to simultaneous scan a whole field of view rather than transmitting focused beams, as in traditional Doppler techniques. The high-frame rate permits up to a 50-fold increase in sensitivity for blood flow changes in the human brain, which correlate neuronal activity as assessed by EEG.[5] In preclinical imaging, cerebral blood volume changes seen on UfD highly correlated with neuronal activity, with a high spatiotemporal resolution of ~100 mm and 1 millisecond.[43,44] Improved sensitivity for slow-flow and smaller vessels is particularly important in rheumatology,[42,45] brain vascular imaging,[46,47] and carotid flow velocity estimation.[48–50]

Note that the super high temporal resolution of UfD surpasses that of functional MRI (fMRI). The high temporal resolution of up to 1 millisecond contrasts with that of traditional fMRI, which is at best 1 second. This has important clinical implications in the neonatal and infant population as fMRI is not routinely performed because of the complexity of the examination, including sedation, transportation,

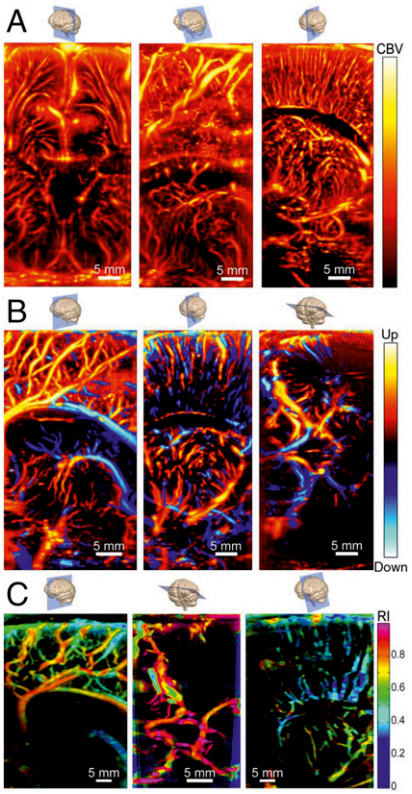

FIGURE 7

UfD images of the normal neonatal brain are shown. A, Ultrafast power Doppler images of the neonatal brain acquired through the anterior fontanel from left to right: coronal view, tilted parasagittal view, parasagittal view. B, Directional power Doppler images based on the speed information from left to right: medial sagittal view revealing venous network around lateral ventricle, parasagittal view revealing small thalamic and cortical arterioles and venules, and transtemporal transverse view through mastoid fontanel for imaging the circle of Willis and cerebellum. C, Resistivity mapping based on UfD data. The RI in big arteries is between 0.8 and 1 (left and center image), whereas the RI in small and veins are lower at ~0.6 and <0.3, respectively. Images reprinted from Demené et al, 2018[51] with permission. CBV, cerebral blood volume; RI, resistivity index.

and high cost. It is also highly convenient for intraoperative use and for continuous, noninvasive monitoring of cerebral function during surgeries. Close bedside monitoring of perfusion changes associated with brain injury and/or seizure activity for children of all ages may be feasible with this technique, although further research is required in this regard. Further studies will be needed, however, to understand the potential correlation between fMRI and UfD because the former measures oxygenated blood whereas the latter measures both oxygenated and deoxygenated blood, technically different physiologic parameters. UfD on the other hand is low cost, portable, and easily repeatable without the need for sedation.

3D AND 4D ULTRASOUND

Although 3D ultrasound suffered from long image-processing times during its infancy, current computer technology allows for high speed of image acquisition and reconstruction. In the 3D technology, positional information gained from the transducer or external positional devices is used to reconstruct 3D images from two-dimensional (2D) images. In the case of hydrocephalus, the traditionally used manual quantification of the ventricular size on a 2D plane is more cumbersome and less accurate than the volumetric reconstruction of the ventricular system (Fig 8).[52–57] The 3D technique is also useful in generating accurate organ or tumor volume.[58] The 4D technology allows for the incorporation of time dimension into 3D imaging, which can be useful in the imaging of moving objects, such as the heart valves. The 3D-4D technique overcomes the limitations of a 2D technique, namely lengthy acquisition times, operator dependence during multiple sweeps, and mental integration of 2D-acquired images. With further developments of 3D-4D technology, simultaneous acquisition of whole-organ perfusion with UfD or CEUS may be possible, which will drastically change the way in which ultrasound is used in the clinical setting. Further improvements will be needed to minimize artifacts associated with 3D-4D technology[59] that may cause diagnostic challenges.

HIGH-FREQUENCY ULTRASOUND

The frequency range of medical ultrasound systems for most scanners is from 2 to 20 MHz. Recently, ultrasound systems of much higher frequency ranges have been

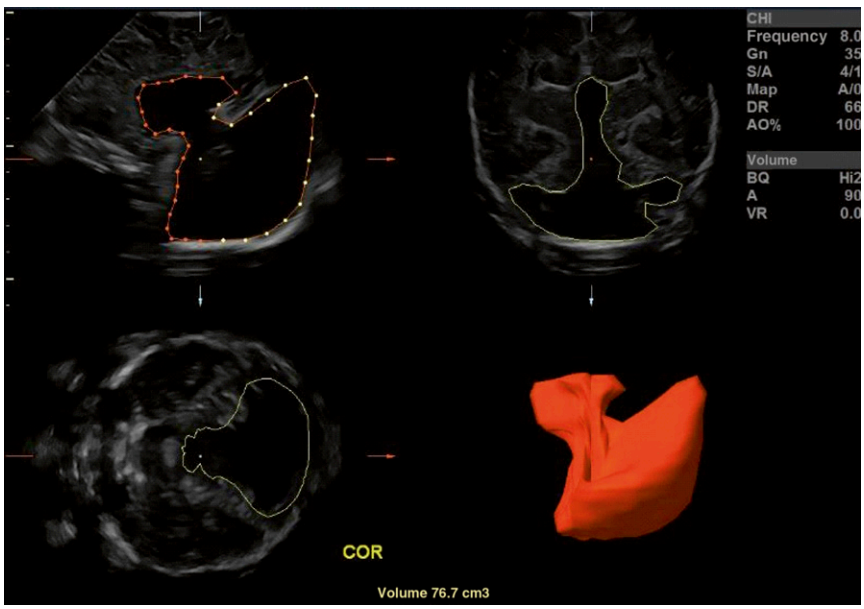

FIGURE 8

A representative image revealing the 3D reconstruction and quantification of the brain ventricular volume. Dotted lines trace the borders of the mildly enlarged third and fourth ventricles in sagittal (top left), axial (bottom left), and coronal planes (top right) for 3D reconstruction (bottom right). The calculated ventricular volume (red) is shown at the bottom. COR, coronal.

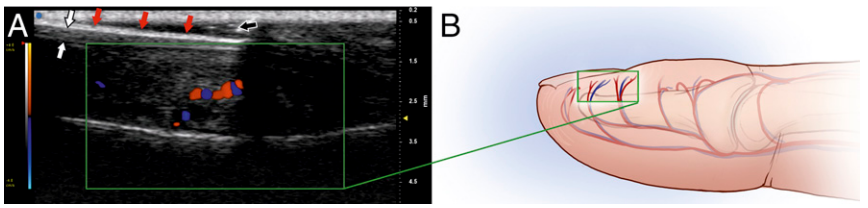

FIGURE 9

The nail plate of the distal phalanx of the second digit was imaged with a high-resolution ultrasound scanner by using a 40 MHz transducer. Shown is the picture diagram of the distal aspect of the second digit (B), with the magnification box noting the region of ultrasound evaluation. Annotated on the corresponding grayscale image (A) are the nail plate of the distal phalanx of the second digit (red arrows), nail bed with germinal matrix (between white arrows), eponychium (cuticle) (black arrow), and vessels supplying the nail unit (inside white box).

introduced to the clinical setting, permitting a significant increase in resolution. VisualSonics ultrahigh-resolution ultrasound systems (FUJIFILM VisualSonics, Inc, Toronto, Canada), used for preclinical studies for the past 10 years, are now FDA approved for clinical applications. Note that the higher frequency peak of up to 70 MHz provides a tremendous increase in resolution compared with that of conventional ultrasound systems, permitting resolution down to 30 μm. Such resolution surpasses that of CT or MRI. Note that an increased frequency results in an increase in ultrasound attenuation in tissues, which means that the use of the system is limited to the first 3 cm of the body. Such resolution can be used to depict single hair follicles growing out of the skin.

The best applications of the high-resolution ultrasound system are neonatology, neuromusculoskeletal, dermatology, lymphatic, vascular, thyroid, and other small-part imaging.[60–66] Further neuromusculoskeletal application of this technique would be helpful for guided superficial nerve blocks or reconstructive surgeries. Higher resolution imaging of the subungual space, moreover, can help assess the integrity of the subungual vessels (terminal branches of the proper digital artery) in the setting of trauma or help characterize various types of benign and malignant tumors affecting the subungual space (Fig 9). A variety of pediatric venous diseases leading to the formation of debris or

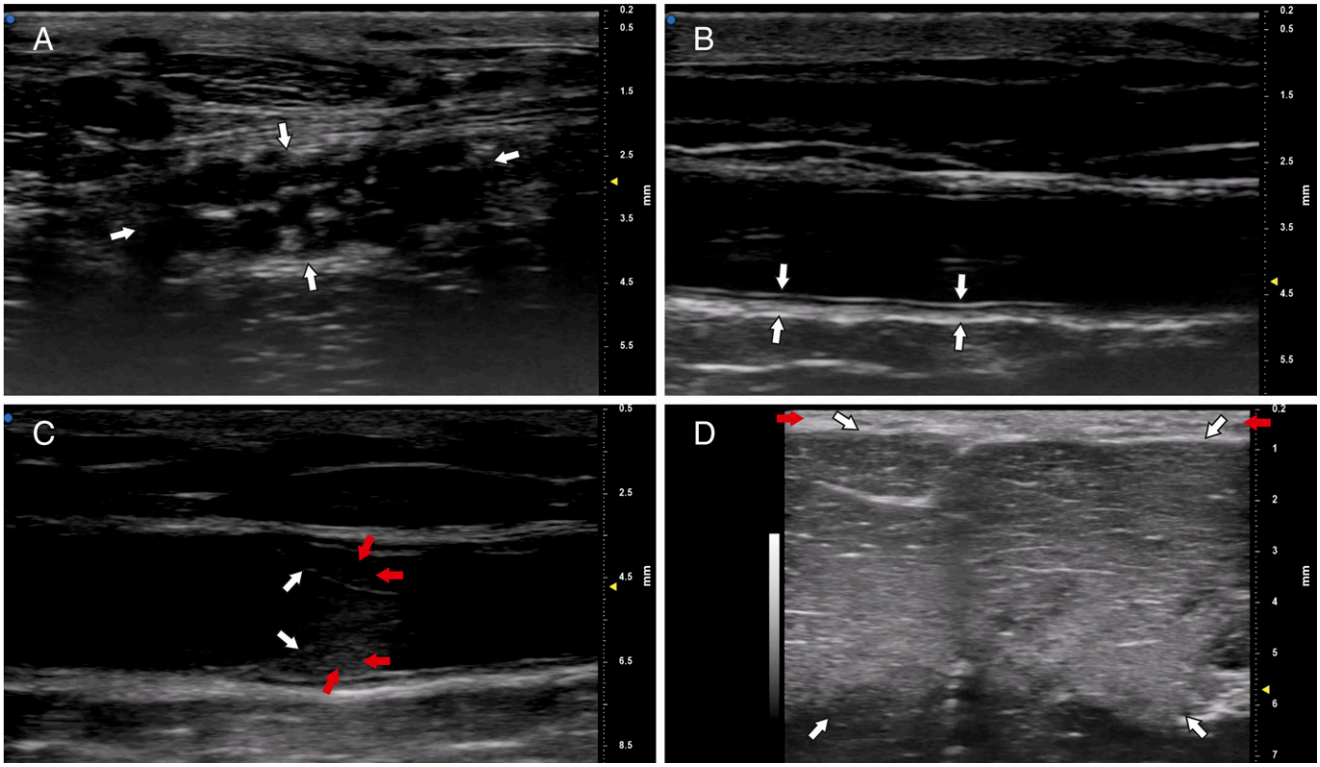

FIGURE 10

Small parts imaged with a high-resolution ultrasound scanner. A, A 50-MHz transducer was used to image the right median nerve in the transverse plane (white arrows) and the numerous fascicles visible within the nerve. B, A 50-MHz transducer was used to image the wall of the superficial palmar arch artery with intima-media (white arrows). C, A 30-MHz transducer was used to image the dilated superficial vein of the lower extremity with the valves (white arrows) and debris in the folds of valves preventing full opening of the valves (red arrows). D, A 50-MHz transducer was used to image the inner oral cavity sublingual glands (white arrows) and the mucous membrane (between red arrows).

thrombus in the superficial and deep veins can be evaluated with high-resolution ultrasound. Other applications include improved characterization of nerve fascicles, large- and small-vessel intima-media thickness, internal contents of peripheral veins, and salivary glands (Fig 10). Thyroid nodules, superficial vascular anomalies, and ocular pathology, especially in small children, would also be better evaluated with high-resolution imaging.

It is important to note that for evaluation of superficial soft-tissue abnormalities in small children, ultrasound provides higher spatial resolution than MRI. The spatial resolution of a high-resolution ultrasound scanner is in micrometers, whereas that of MRI is in millimeters. With the availability of FDA-approved ultrasound contrast, ultrasound can now provide dynamic enhancement information similar to multiphase contrast-enhanced MRI. Moreover, sedation required for MRI of most small children is not without risks. Although the diagnostic benefits of MRI should be acknowledged, the awareness that, in some circumstances, advanced ultrasound techniques can provide the necessary diagnostic information is worth noting. In referral of pediatric patients to radiologic exams, such knowledge would be beneficial.

CONCLUSIONS AND FUTURE DIRECTIONS

Rapid advancements in ultrasound techniques are changing the role of ultrasound in the management of a pediatric patient. Ultrasound is not merely a screening tool that precedes cross-sectional examinations; it is a critical tool in disease diagnosis and monitoring as well as therapeutic guidance, including as a point-of-care modality. The aforementioned techniques now offer functional information, including dynamic perfusion, tissue stiffness, and hemodynamic changes at the spatiotemporal resolution surpassing that of MRI. Improved 3D-4D and high-resolution techniques additionally serve to enhance the diagnostic potential of ultrasound. Combined with portability, low cost, lack of the need for radiation and sedation, and safety, ultrasound in which advanced techniques are used can serve as a useful clinical tool in the management of pediatric patients.

Further research in validating the emerging ultrasound techniques is ongoing. CEUS, for instance, is increasingly being explored for novel applications besides focal liver lesions and vesicoureteral reflux. In the case of elastography, the exact histopathologic and physiologic mechanisms behind changes in quantitatively measured tissue stiffness warrant further study. The continued work in this regard will improve our understanding of the parameters measured with advanced ultrasound techniques and help generate standardized guidelines to help discern healthy from diseased and/or injured organs.

ABBREVIATIONS

2D: two-dimensional
3D: three-dimensional
4D: four-dimensional
CEUS: contrast-enhanced ultrasound
ceVUS: contrast-enhanced voiding urosonography
CT: computed tomography
FDA: Food and Drug Administration
fMRI: functional MRI
UfD: ultrafast Doppler
VCUG: voiding cystourethrography

REFERENCES

1. Hwang M, De Jong RM Jr, Herman S, et al. Novel contrast-enhanced ultrasound evaluation in neonatal hypoxic ischemic injury: clinical application and future directions. *J Ultrasound Med*. 2017;36(11):2379–2386
2. Hwang M, Riggs BJ, Katz J, et al. Advanced pediatric neurosonography techniques: contrast-enhanced ultrasonography, elastography, and beyond. *J Neuroimaging*. 2018;28(2):150–157
3. Hwang M, Sridharan A, Darge K, et al. Novel quantitative contrast-enhanced ultrasound detection of hypoxic ischemic injury in neonates and infants [published online ahead of print December 17, 2018]. *Pilot Study*. 2018; doi:10.1002/jum.14892
4. Light ED, Mukundan S, Wolf PD, Smith SW. Real-time 3-d intracranial ultrasound with an endoscopic matrix array transducer. *Ultrasound Med Biol*. 2007;33(8):1277–1284
5. Demene C, Baranger J, Bernal M, et al. Functional ultrasound imaging of brain activity in human newborns. *Sci Transl Med*. 2017;9(411):eaah6756
6. US Food and Drug Administration. Drugs@FDA: FDA approved drug products–Lumason. 2016. Available at: https://www.accessdata.fda.gov/scripts/cder/daf/index.cfm?event=overview.process'appno=203684. Accessed January 12, 2019
7. Piscaglia F, Bolondi L; Italian Society for Ultrasound in Medicine and Biology (SIUMB) Study Group on Ultrasound Contrast Agents. The safety of Sonovue in abdominal applications: retrospective analysis of 23188 investigations. *Ultrasound Med Biol*. 2006;32(9):1369–1375
8. Piskunowicz M, Kosiak W, Batko T, Piankowski A, Połczyńska K, Adamkiewicz-Drożyńska E. Safety of intravenous application of second-generation ultrasound contrast agent in children: prospective analysis. *Ultrasound Med Biol*. 2015;41(4):1095–1099
9. Thimm MA, Rhee D, Takemoto CM, et al. Diagnosis of congenital and acquired focal lesions in the neck, abdomen, and pelvis with contrast-enhanced ultrasound: a pictorial essay. *Eur J Pediatr*. 2018;177(10):1459–1470
10. Bilotta F, Evered LA, Gruenbaum SE. Neurotoxicity of anesthetic drugs: an

update. *Curr Opin Anaesthesiol*. 2017; 30(4):452–457

11. Houck CS, Vinson AE. Anaesthetic considerations for surgery in newborns. *Arch Dis Child Fetal Neonatal Ed*. 2017;102(4):F359–F363
12. Claudon M, Dietrich CF, Choi BI, et al. Guidelines and good clinical practice recommendations for contrast enhanced ultrasound (CEUS) in the liver–update 2012: a WFUMB-EFSUMB initiative in cooperation with representatives of AFSUMB, AIUM, ASUM, FLAUS and ICUS. *Ultraschall Med*. 2013;34(1):11–29
13. Murphy-Lavallee J, Jang HJ, Kim TK, Burns PN, Wilson SR. Are metastases really hypovascular in the arterial phase? The perspective based on contrast-enhanced ultrasonography. *J Ultrasound Med*. 2007;26(11): 1545–1556
14. Gonda T, Ishida H, Yoshinaga K, Sugihara K. Microvasculature of small liver metastases in rats. *J Surg Res*. 2000;94(1):43–48
15. Jang HJ, Yu H, Kim TK. Contrast-enhanced ultrasound in the detection and characterization of liver tumors. *Cancer Imaging*. 2009;9:96–103
16. Yusuf GT, Sellars ME, Deganello A, Cosgrove DO, Sidhu PS. Retrospective analysis of the safety and cost implications of pediatric contrast-enhanced ultrasound at a single center. *AJR Am J Roentgenol*. 2017;208(2): 446–452
17. Hwang M, Riggs BJ, Saade-Lemus S, Huisman TA. Bedside contrast-enhanced ultrasound diagnosing cessation of cerebral circulation in a neonate: a novel bedside diagnostic tool. *Neuroradiol J*. 2018;31(6):578–580
18. Miele V, Piccolo CL, Galluzzo M, Ianniello S, Sessa B, Trinci M. Contrast-enhanced ultrasound (CEUS) in blunt abdominal trauma. *Br J Radiol*. 2016;89(1061): 20150823
19. Armstrong LB, Mooney DP, Paltiel H, et al. Contrast enhanced ultrasound for the evaluation of blunt pediatric abdominal trauma. *J Pediatr Surg*. 2018;53(3):548–552
20. Quaia E, Gennari AG, Cova MA, van Beek EJR. Differentiation of inflammatory from fibrotic ileal strictures among patients with Crohn's disease based on visual analysis: feasibility study combining conventional B-mode ultrasound, contrast-enhanced ultrasound and strain elastography. *Ultrasound Med Biol*. 2018;44(4): 762–770
21. Coelho R, Ribeiro H, Maconi G. Bowel thickening in Crohn's disease: fibrosis or inflammation? Diagnostic ultrasound imaging tools. *Inflamm Bowel Dis*. 2017; 23(1):23–34
22. Papadopoulou F, Ntoulia A, Siomou E, Darge K. Contrast-enhanced voiding urosonography with intravesical administration of a second-generation ultrasound contrast agent for diagnosis of vesicoureteral reflux: prospective evaluation of contrast safety in 1,010 children. *Pediatr Radiol*. 2014;44(6): 719–728
23. Piskunowicz M, Świętoń D, Rybczyńska D, et al. Comparison of voiding cystourethrography and urosonography with second-generation contrast agents in simultaneous prospective study. *J Ultrason*. 2016;16(67):339–347
24. Mane N, Sharma A, Patil A, Gadekar C, Andankar M, Pathak H. Comparison of contrast-enhanced voiding urosonography with voiding cystourethrography in pediatric vesicoureteral reflux. *Turk J Urol*. 2018; 44(3):261–267
25. Benedito J, Carcel JA, Sanjuan N, Mulet A. Use of ultrasound to assess Cheddar cheese characteristics. *Ultrasonics*. 2000;38(1–8):727–730
26. Yeh WC, Li PC, Jeng YM, et al. Elastic modulus measurements of human liver and correlation with pathology. *Ultrasound Med Biol*. 2002;28(4): 467–474
27. Sandrin L, Fourquet B, Hasquenoph JM, et al. Transient elastography: a new noninvasive method for assessment of hepatic fibrosis. *Ultrasound Med Biol*. 2003;29(12):1705–1713
28. Castéra L, Vergniol J, Foucher J, et al. Prospective comparison of transient elastography, Fibrotest, APRI, and liver biopsy for the assessment of fibrosis in chronic hepatitis C. *Gastroenterology*. 2005;128(2):343–350
29. Friedrich-Rust M, Ong MF, Martens S, et al. Performance of transient elastography for the staging of liver fibrosis: a meta-analysis. *Gastroenterology*. 2008;134(4):960–974
30. Tsochatzis EA, Gurusamy KS, Ntaoula S, Cholongitas E, Davidson BR, Burroughs AK. Elastography for the diagnosis of severity of fibrosis in chronic liver disease: a meta-analysis of diagnostic accuracy. *J Hepatol*. 2011;54(4):650–659
31. Cardoso AC, Carvalho-Filho RJ, Stern C, et al. Direct comparison of diagnostic performance of transient elastography in patients with chronic hepatitis B and chronic hepatitis C. *Liver Int*. 2012;32(4): 612–621
32. Sporea I, Sirli R, Deleanu A, et al. Liver stiffness measurements in patients with HBV vs HCV chronic hepatitis: a comparative study. *World J Gastroenterol*. 2010;16(38):4832–4837
33. Chon YE, Choi EH, Song KJ, et al. Performance of transient elastography for the staging of liver fibrosis in patients with chronic hepatitis B: a meta-analysis. *PLoS One*. 2012;7(9): e44930
34. Mahadeva S, Mahfudz AS, Vijayanathan A, Goh KL, Kulenthran A, Cheah PL. Performance of transient elastography (TE) and factors associated with discordance in non-alcoholic fatty liver disease. *J Dig Dis*. 2013;14(11):604–610
35. Kumar R, Rastogi A, Sharma MK, et al. Liver stiffness measurements in patients with different stages of nonalcoholic fatty liver disease: diagnostic performance and clinicopathological correlation. *Dig Dis Sci*. 2013;58(1):265–274
36. Andersen SB, Ewertsen C, Carlsen JF, Henriksen BM, Nielsen MB. Ultrasound elastography is useful for evaluation of liver fibrosis in children-a systematic review. *J Pediatr Gastroenterol Nutr*. 2016;63(4):389–399
37. Cholongitas E, Senzolo M, Standish R, et al. A systematic review of the quality of liver biopsy specimens. *Am J Clin Pathol*. 2006;125(5):710–721
38. Regev A, Berho M, Jeffers LJ, et al. Sampling error and intraobserver variation in liver biopsy in patients with chronic HCV infection. *Am J Gastroenterol*. 2002;97(10):2614–2618
39. deCampo D, Hwang M. Characterizing the neonatal brain with ultrasound

elastography. *Pediatr Neurol*. 2018;86: 19–26

40. Dillman JR, Stidham RW, Higgins PD, et al. Ultrasound shear wave elastography helps discriminate low-grade from high-grade bowel wall fibrosis in ex vivo human intestinal specimens. *J Ultrasound Med*. 2014; 33(12):2115–2123
41. Lin HY, Lee YL, Lin KD, et al. Association of renal elasticity and renal function progression in patients with chronic kidney disease evaluated by real-time ultrasound elastography. *Sci Rep*. 2017; 7:43303
42. Tanter M, Fink M. Ultrafast imaging in biomedical ultrasound. *IEEE Trans Ultrason Ferroelectr Freq Control*. 2014; 61(1):102–119
43. Macé E, Montaldo G, Cohen I, Baulac M, Fink M, Tanter M. Functional ultrasound imaging of the brain. *Nat Methods*. 2011;8(8):662–664
44. Osmanski BF, Martin C, Montaldo G, et al. Functional ultrasound imaging reveals different odor-evoked patterns of vascular activity in the main olfactory bulb and the anterior piriform cortex. *Neuroimage*. 2014;95:176–184
45. Maresca D, Tanter M, Pernot M. Ultrasound microangiography of the metacarpophalangeal joint using ultrafast Doppler. In: Proceedings From the Institute of Electrical and Electronics Engineers International Ultrasonics Symposium; September 3–6, 2014; Chicago, IL
46. Demené C, Pernot M, Biran V, et al. Ultrafast Doppler reveals the mapping of cerebral vascular resistivity in neonates. *J Cereb Blood Flow Metab*. 2014;34(6):1009–1017
47. Demené C, Tiran E, Sieu LA, et al. 4D microvascular imaging based on ultrafast Doppler tomography. *Neuroimage*. 2016;127:472–483
48. Ekroll IK, Voormolen MM, Standal OK, Rau JM, Lovstakken L. Coherent compounding in doppler imaging. *IEEE Trans Ultrason Ferroelectr Freq Control*. 2015;62(9):1634–1643
49. Hasegawa H, Kanai H. Simultaneous imaging of artery-wall strain and blood flow by high frame rate acquisition of RF signals. *IEEE Trans Ultrason Ferroelectr Freq Control*. 2008;55(12): 2626–2639
50. Lenge M, Ramalli A, Boni E, Liebgott H, Cachard C, Tortoli P. High-frame-rate 2-D vector blood flow imaging in the frequency domain. *IEEE Trans Ultrason Ferroelectr Freq Control*. 2014;61(9): 1504–1514
51. Demene C, Mairesse J, Baranger J, et al. Ultrafast Doppler for neonatal brain imaging. *Neuorimage*. 2019;185(15): 851–856
52. Riccabona M, Nelson TR, Weitzer C, Resch B, Pretorius DP. Potential of three-dimensional ultrasound in neonatal and paediatric neurosonography. *Eur Radiol*. 2003; 13(9):2082–2093
53. Nagdyman N, Walka MM, Kampmann W, Stöver B, Obladen M. 3-D ultrasound quantification of neonatal cerebral ventricles in different head positions. *Ultrasound Med Biol*. 1999;25(6): 895–900
54. Abdul-Khaliq H, Lange PE, Vogel M. Feasibility of brain volumetric analysis and reconstruction of images by transfontanel three-dimensional ultrasound. *J Neuroimaging*. 2000;10(3): 147–150
55. Csutak R, Unterassinger L, Rohrmeister C, Weninger M, Vergesslich KA. Three-dimensional volume measurement of the lateral ventricles in preterm and term infants: evaluation of a standardised computer-assisted method in vivo. *Pediatr Radiol*. 2003; 33(2):104–109
56. Gilmore JH, Gerig G, Specter B, et al. Infant cerebral ventricle volume: a comparison of 3-D ultrasound and magnetic resonance imaging. *Ultrasound Med Biol*. 2001;27(8): 1143–1146
57. Kampmann W, Walka MM, Vogel M, Obladen M. 3-D sonographic volume measurement of the cerebral ventricular system: in vitro validation. *Ultrasound Med Biol*. 1998;24(8): 1169–1174
58. Pflanzer R, Hofmann M, Shelke A, et al. Advanced 3D-sonographic imaging as a precise technique to evaluate tumor volume. *Transl Oncol*. 2014;7(6):681–686
59. Nelson TR, Downey DB, Pretorius DH, Fenster A, eds. *Three-Dimensional Ultrasound*. Philadelphia, PA: Lippincott Williams ' Wilkins; 1999
60. Viviano SL, Chandler LK, Keith JD. Ultrahigh frequency ultrasound imaging of the hand: a new diagnostic tool for hand surgery. *Hand (N Y)*. 2018; 13(6):720–725
61. Visconti G, Hayashi A, Yoshimatsu H, Bianchi A, Salgarello M. Ultra-high frequency ultrasound in planning capillary perforator flaps: preliminary experience. *J Plast Reconstr Aesthet Surg*. 2018;71(8):1146–1152
62. Dangardt F, Charakida M, Chiesa S, et al. Intimal and medial arterial changes defined by ultra-high-frequency ultrasound: response to changing risk factors in children with chronic kidney disease. *PLoS One*. 2018;13(6):e0198547
63. Hayashi A, Visconti G, Yamamoto T, et al. Intraoperative imaging of lymphatic vessel using ultra high-frequency ultrasound. *J Plast Reconstr Aesthet Surg*. 2018;71(5):778–780
64. Cartwright MS, Baute V, Caress JB, Walker FO. Ultrahigh-frequency ultrasound of fascicles in the median nerve at the wrist. *Muscle Nerve*. 2017; 56(4):819–822
65. Botar-Jid CM, Cosgarea R, Bolboacă SD, et al. Assessment of cutaneous melanoma by use of very- high-frequency ultrasound and real-time elastography. *AJR Am J Roentgenol*. 2016;206(4):699–704
66. Berritto D, Iacobellis F, Rossi C, Reginelli A, Cappabianca S, Grassi R. Ultra high-frequency ultrasound: new capabilities for nail anatomy exploration. *J Dermatol*. 2017;44(1):43–46